

**HHS PUBLIC ACCESS**

Author manuscript

ACS Infect Dis. Author manuscript; available in PMC 2017 May 01.

Published in final edited form as:

ACS Infect Dis. 2017 February 10; 3(2): 176–181. doi:10.1021/acinfecdis.6b00172.

**Rational Design of Selective and Bioactive Inhibitors of the *Mycobacterium tuberculosis* Proteasome**Kyle A. Totaro<sup>†</sup>, Dominik Barthelme<sup>‡</sup>, Peter T. Simpson<sup>†</sup>, Xiujiu Jiang<sup>§</sup>, Gang Lin<sup>§</sup>, Carl F. Nathan<sup>§</sup>, Robert T. Sauer<sup>†</sup>, and Jason K. Sello<sup>\*,†</sup><sup>†</sup>Department of Chemistry, Brown University, 324 Brook Street, Box H, Providence, RI 02912, United States<sup>‡</sup>Department of Biology, Massachusetts Institute of Technology, 77 Massachusetts Avenue, 68-571A, Cambridge, MA 02139, United States<sup>§</sup>Department of Microbiology and Immunology, Weill Cornell Medicine, 1300 York Avenue, New York, NY 10065, United States**Abstract**

The 20S core particle of the proteasome in *M. tuberculosis* (*Mtb*) is a promising, yet unconventional drug target. This multimeric peptidase is not essential, yet degrades proteins that have become damaged and toxic via reactions with nitric oxide (and/or the associated reactive nitrogen intermediates) produced during the host immune response. Proteasome inhibitors could render *Mtb* susceptible to the immune system, but they would only be therapeutically viable if they do not inhibit the essential 20S counterpart in humans. We designed and synthesized selective inhibitors of the *Mtb* 20S based on both its unique substrate preferences and the structures of substrate-mimicking covalent inhibitors of eukaryotic proteasomes called syringolins. Unlike the parent syringolins, the designed analogs weakly inhibit the human 20S (*Hs* 20S) proteasome and preferentially inhibit *Mtb* 20S over the human counterpart by as much as 74-fold. Moreover, they can penetrate the mycobacterial cell envelope and render *Mtb* susceptible to nitric oxide-mediated stress. Importantly, they do not inhibit the growth of human cell lines *in vitro* and thus may be starting points for tuberculosis drug development.

**Keywords**

syringolins; peptidomimetic; protein homeostasis; innate immune response; nitric oxide; host-pathogen interaction

---

<sup>\*</sup>Corresponding Author: [jason\\_sello@brown.edu](mailto:jason_sello@brown.edu).**Supporting Information.** The Supporting Information is available free of charge on the ACS Publications website. Supporting figures, procedures, and <sup>1</sup>H and <sup>13</sup>C NMR spectra (PDF)**Author Contributions**

All authors have given approval to the final version of the manuscript.

**DEDICATION**

This manuscript is dedicated to Professor Stuart Lee Schreiber on the occasion of his sixtieth birthday.

*Mycobacterium tuberculosis* (*Mtb*), the deadliest bacterial pathogen, is increasingly dangerous because of drug resistance and is thus the focus of drug-development programs.<sup>1,2</sup> Among recently identified potential drug targets of *Mtb*, the 20S peptidase of the proteasome (*Mtb* 20S) is unusual.<sup>3,4</sup> It is distinct from many drug targets in that it is only conditionally required for viability. *Mtb* mutants lacking the enzyme are viable *in vitro*, but cannot sustain an infection in an animal model of tuberculosis.<sup>3</sup> Within mammalian hosts, *Mtb* 20S is essential for the bacterium to survive exposure to the nitric oxide produced by macrophages and other cells of the innate immune system.<sup>3,4</sup> Presumably, proteins that could become toxic via damage by reactions with either nitric oxide or the reactive nitrogen intermediates derived from it are targeted for proteasome-mediated degradation via a post-translational modification with the prokaryotic ubiquitin-like protein, the functional equivalent of ubiquitin in eukaryotes.<sup>5</sup> This presumption has been validated by reports that *Mtb* 20S inhibitors, like null mutations in the proteasome gene, sensitize *Mtb* to nitric oxide.<sup>3,6-9</sup> This chemical validation gives credence to an unconventional pharmacological strategy in which small molecules are not used to kill *Mtb*, but to render it susceptible to the immune response.

A potential liability of this strategy for pharmacologically intervening in the host-pathogen interaction is that *Mtb* 20S is similar in structure to and has the same catalytic mechanism as the essential human 20S.<sup>3,6-9</sup> Indeed, the 20S peptidases of *Mtb* and eukaryotes share a barrel-shaped  $\alpha_7\beta_7\beta_7\alpha_7$  structure and have a catalytic, N-terminal threonine residue. Though they are structurally related, the catalytic  $\beta$ -subunits in eukaryotes have three different isoforms exhibiting distinct substrate specificities, while those in the *Mtb* are identical.<sup>10,11</sup> In analogy to anti-cancer drugs that inhibit human 20S, *Mtb* 20S inhibitors could be therapeutic agents for tuberculosis.<sup>10,11</sup> However, inhibitors of the *Mtb* 20S will only have the safety profile for therapeutic use if they are species-selective.

Progress towards the development of selective inhibitors of *Mtb* 20S has been enabled by knowledge of the unique substrate preferences<sup>7</sup> and structural features<sup>9</sup> of the enzyme. Reflecting the peculiarities of its S1 and S3 pockets, *Mtb* 20S strongly prefers substrates with a bulky tryptophan residue at the P1 position and either glycine or proline at the P3 position, respectively.<sup>7,9,12</sup> With this information, an analog of the proteasome inhibiting cancer drug Bortezomib (Velcade) having a *meta*-chlorobenzyl moiety mimicking the preferred substrate's tryptophan residue at P1 was designed and reported to be an 8-fold selective inhibitor of *Mtb* 20S.<sup>7</sup> By extension, we proposed that molecules mimicking both the P1 and P3 residues of the enzyme's preferred substrates would be even more selective. We then examined the structures of peptidomimetic 20S inhibitors from the cancer drug development literature as scaffolds for the design of compounds that could selectively inhibit *Mtb* 20S.<sup>13</sup> Our key criteria for scaffold selection were: a covalent mode of inhibition that would potentially circumvent the problematic off-target effects of reversible inhibitors like Bortezomib<sup>14</sup> and a well-defined mode of binding to the proteasome. Hence, we selected the syringolin natural products derived from *Pseudomonas syringae*. (Figure 1).<sup>15,16</sup> Their enamide moiety undergoes an irreversible conjugate addition with the active site threonine of the peptidase.<sup>15</sup> In the crystal structure of yeast 20S with a covalently bound syringolin A adduct,<sup>16</sup> the macrolactam's isopropyl substituent and the side chain of the valine residue in the appendant ureido peptide moiety fit into the S1 and S3 pockets of the active site,

respectively.<sup>16,17</sup> We reasoned that replacement of the substituents of the macrolactam and the ureido peptide moiety with structures that are analogous to the side chains of the amino acids at the P1 (*i.e.*, tryptophan) and P3 (*i.e.*, glycine or proline) positions of a preferred *Mtb* 20S substrate would yield a species-selective inhibitor (Figure 2). Beyond the structure-based design considerations, we selected the syringolins because they facilitate the capacity of *P. syringae* to infect plants.<sup>15,17</sup> Because these molecules can penetrate the thick cell wall of plants, we predicted that analogs would have a high likelihood of traversing the notoriously exclusive cell envelope of *M. tuberculosis* and thus be active against the bacterium *in vitro* and *in vivo*.

To prepare the envisioned syringolin analogs, we utilized a diversity-oriented, modular synthetic scheme inspired by the work of Stephenson<sup>18</sup> and Pirrung<sup>19</sup> and recently reported by us<sup>20</sup> (Scheme 1). In addition to macrolactams having a methyl indole moiety like that of tryptophan, we prepared compounds having substituted benzyl groups like those of the aforementioned, selective inhibitor of *Mtb* 20S.<sup>7</sup> Macrolactams having an unsubstituted benzyl group and the isopropyl substituent of the syringolin natural products were prepared as negative controls because the *Mtb* 20S has low turnover rates for substrates with phenylalanine and aliphatic amino acids at the P1 position, respectively. The macrolactams having various substituents at the R position were functionalized in a convergent fashion with ureido building blocks having various amino acids at the R' site, mimicking the P3 residue of the substrate. Though *Mtb* 20S strongly prefers substrates with proline or glycine at this position, we prepared compounds with other amino acids to test the models for substrate preference and mimicry. In all of our syringolin analogs (Table 1; Fig. 2), the carboxylic acid of the ureido peptide side chain was transformed to a methyl ester, as this modification improves bioactivity of syringolin A.<sup>21</sup>

To assess the potencies and selectivities of the syringolin analogs as proteasome inhibitors, we incubated them with either human or *Mtb* 20S and subsequently measured the rates of enzyme-catalyzed hydrolysis of a fluorogenic substrate (Suc-LLVY-AMC). Because this substrate is well-behaved and soluble, it is widely used in kinetic analyses of both human and *Mtb* 20S activities. As irreversible inhibitors, the syringolin analogs were expected to react with 20S in a time-dependent fashion in enzymatic assays. Thus, various concentrations of the inhibitors were added to mixtures of the enzyme and the fluorogenic substrate and then the rates of hydrolysis of the fluorogenic substrate were measured continuously and used to determine second-order rate constants for inhibition,  $k_{in}/K_i$  ( $M^{-1}s^{-1}$ ) (Table 1) (see supporting information). As these measurements reflect the affinity of the non-covalent binding ( $K_i$ ) and the rate of the chemical reaction of the inhibitors with the enzyme ( $k_{in}$ ), direct comparisons of the compounds can be made. Further, the ratios of the second-order rate constants for inhibition of the human and *Mtb* 20S were used to calculate the degree of species selectivity.

All syringolin analogs inhibited the catalytic activities of both enzymes, but there were distinct reactivity trends that were congruent with the model for peptidomimicry by the syringolins and the substrate preferences *Mtb* 20S (Table 1). As anticipated, replacement of the isopropyl substituent on the syringolin B macrolactam (Table 1, compound 1) with aromatic moieties (Table 1, compounds 2-12) consistently led to improvements in second-

order inhibition rates for *Mtb* 20S. Gratifyingly, the most reactive inhibitor of this enzyme had the tryptophan side chain at R (Table 1, compound 12). Though compounds with aromatic moieties at R were generally better inhibitors of human 20S, a 127-fold improvement in species-selectivity was observed (Table 1, compound 1 vs. 12). However, none of these compounds exhibited preferential inhibition of *Mtb* 20S.

Having established that inclusion of the methyl indole side chain of tryptophan on the macrolactam improved selectivity for *Mtb* 20S, we explored modifications of the amino acid in the appendant ureido side-chain substituent ( $R'$  in Figure 2). Importantly and consistent with our design strategy, compounds with either proline (Table 1, compound 13) or glycine (Table 1, compound 14) at that position preferentially inhibited *Mtb* 20S- the former and latter were 33- and 74-fold selective for the *Mtb* 20S, respectively. We also note that the most selective inhibitor is 220-fold more reactive with *Mtb* 20S than the parent compound (Table 1, compound 1). Surprisingly, a compound designed to mimic a poor substrate of the *Mtb* 20S proteasome (*i.e.*, a peptide with phenylalanine at P3)<sup>7</sup> was highly reactive with the enzyme; however, it preferentially inhibited the human enzyme (Table 1, compound 16). Collectively, these results indicate that the mimic of the substrate's P3 residue is especially important for defining species-selectivity.

To gain further insights into the structure-activity relationships, we carried out additional experiments. Because syringolin A, defined by an additional unit of unsaturation in the macrolactam, was reportedly more potent than syringolin B,<sup>15,16,21–23</sup> we prepared an analog of the most selective inhibitor with this moiety and found that it had a higher degree of reactivity; it was less species-selective. In addition, we synthesized an analog of our most selective inhibitor (Table 1, compound 14) having a *N,N*-diethyl asparagine side chain at  $R'$  (Table 1, compound 17), which was reported as a good P3 mimic in the structure of a highly selective *N,C*-capped dipeptide inhibitor of *Mtb* 20S.<sup>9</sup> We found that this alteration dramatically improved potency, but compromised species-selectivity. We also prepared an analog of the less selective inhibitor (Table 1, compound 13) with homoproline in place of proline (Table 1, compound 18). Apparently, the change in conformation resulting from expansion of the ring dramatically reduced both potency and selectivity for inhibition of *Mtb* 20S. Finally, because the ureido moiety in all of the syringolins could be important for hydrogen bonding to the enzyme, we prepared analogs of our most selective inhibitor (Table 1, compound 14) with either sarcosine or  $\beta$ -alanine in place of glycine. The former enabled assessment of the ureido group's role as a hydrogen bond donor via its *N*-methyl group, whereas the latter allowed analysis of the ureido group's position as a hydrogen-bond donor/acceptor due to its additional methylene. In technically simple yet less precise assays wherein the  $IC_{50}$  of the compounds rather than their second-order rate constants of inhibition were measured, we found that both modifications compromised potency and species-selectivity (data not shown, see supporting information). These observations indicate that the structure and position of the ureido moiety are important for the compounds' enzyme binding.

Based on the bioactivity of the syringolins as virulence factors in plants, we predicted that the analogs would be able to traverse the highly exclusive peptidoglycan of *M. tuberculosis* and inhibit activity of the cytosolic enzyme. To test this prediction, we treated cultures of

*Mycobacterium bovis* BCG (a non-pathogenic surrogate of *M. tuberculosis*) with the most selective inhibitors of *Mtb* 20S (Table 1, compound 13 and 14) and then measured the proteasome-specific activity using a chromogenic substrate after whole cell lysis (Figure 3). While we were gratified to find that the selective inhibitors suppressed the apparent proteasome activity, our finding that the lesser selective inhibitor in the proteasome inhibition assays (compound 13) was the most active in cells was surprising. We ascribe these observations to differences in the compounds' cell permeability; indeed, compound 13 (having proline rather than glycine as a P3 mimic) is more lipophilic than compound 14. Subsequently, we carried out experiments to determine if the compounds would render non-replicating *Mtb* susceptible to nitric oxide in a dose-dependent fashion.<sup>3,8,9</sup> As anticipated, the inhibitors exhibited a dose-dependent bactericidal effect in media supplemented with a source of nitric oxide and had little toxicity in the absence of nitric oxide wherein proteasome activity is not essential for viability (Figure 4). Negative results observed with compound 13<sup>sat</sup> (in which the reactive  $\alpha,\beta$ -enamide required for covalent inhibition had been chemically inactivated by reduction) confirmed the inhibitors' mode of action. Though both inhibitors effected dose-dependent susceptibility of *Mtb* to sodium nitrite, the bactericidal activity of compound 13 plateaued at a higher concentration than compound 14 for reasons that are not obvious (Figure 4). Nevertheless, compound 14, the most potent and selective inhibitor of *Mtb* 20S *in vitro*, was the most efficacious in sensitizing the bacterium to nitrosative stress. In fact, at the highest concentration tested (50  $\mu$ M), this compound effected a three-order of magnitude reduction in the number of colony forming units (CFU) on media supplemented with sodium nitrite (Figure 4).

Because the selective inhibitors of *Mtb* 20S had low reactivity with human 20S, we predicted that they would not have the parent compound's toxicity to human cells (Table 1, compounds 1, 13, and 14). Indeed, we found that, unlike compound 1 (syringolin B methyl ester), compounds 13 and 14 were not toxic to the HepG2 human liver carcinoma cell line at concentrations as high as 50  $\mu$ M (see supporting information). Syringolin B methyl ester and compound 14 were further tested against the National Cancer Institute panel of sixty human cancer cell lines. The mean growth in the presence of compound 14 at 10  $\mu$ M compared to that of the untreated controls was 102%. In contrast, cancer cells exposed to syringolin B methyl ester at the same concentration exhibited 27% of the growth of the cells that were only treated with the vehicle (see supporting information).

Here, we report the rational design and syntheses of species-selective inhibitors of *Mtb* 20S based on the enzyme's substrate preferences and the proposed mode by which the syringolins bind the eukaryotic proteasome. Our approach stands in marked contrast to previous reports in which highly selective inhibitors of *Mtb* 20S were identified via high-throughput screening.<sup>8,9</sup> Though the oxathiazolones and the N,C-capped dipeptides discovered via those high-throughput screening efforts were highly selective (~1300 and ~4,600-fold, respectively) and bioactive, their development into first-in-class tuberculosis drug leads is contingent on optimization of their pharmacological properties. The efforts described herein were motivated by a need to fill this innovation gap in the development of tuberculosis drugs that act via intervention in the host-pathogen interaction. Remarkably, we achieved an absolute inversion in the syringolins' inherent species-selectivity that was accompanied by the virtual elimination of parent compounds' toxicity to human cells.

Relative to the inhibitory parameters of the syringolin B natural product, our most selective inhibitor has a 250-fold improved rate of reaction with *Mtb* 20S and a 99.6% lower rate of reaction with human 20S. Beyond being the first time that a natural product structure was used in the design of a species-selective proteasome inhibitor, our findings are noteworthy because the species-selectivity of our best inhibitor (74-fold preference for *Mtb* 20S) and the degree of change in species-selectivity relative to the starting scaffold (syringolin B has a 160-fold preference for *Hs* 20S) are markedly superior to those achieved in the previous report of structure-based design.<sup>7</sup> In that case, only 8-fold selectivity for *Mtb* 20S inhibition was attained by applying the substrate-guided design strategy to the structure of the cancer drug bortezomib (a synthetic peptide boronate having an 18-fold preference for reversible inhibition of human 20S).<sup>7</sup> More broadly, we note that this substrate-guided design strategy could be applied to most known eukaryotic 20S inhibitors. In fact, it has been recently applied to vinyl sulfones for the development of species-selective inhibitors of the 20S enzyme in *Plasmodium falciparum*, the causative agent of malaria.<sup>24</sup> In any case, our findings validate the peptidomimetic model for enzyme inhibition by the syringolins, provide further validation for the use of *Mtb* 20S inhibitors as selective bactericidal agents, and justify rational design as an alternative to the high-throughput screening methods that have previously been used to identify selective inhibitors of *Mtb* 20S.<sup>10,11</sup> Efforts are now underway to characterize the pharmacokinetic/pharmacodynamic properties of these inhibitors, to further optimize their structures, and to assess their efficacies in animal models of tuberculosis.

## Supplementary Material

Refer to Web version on PubMed Central for supplementary material.

## Acknowledgments

Expert technical support on NMR and mass spectrometry were provided by R. Hopson and T. Shen in the Brown University Department of Chemistry.

### Funding Sources

This work was supported by funding from Brown University and an award from the Lura Cook Hull Trust to JKS. PTS was the recipient of an UTRA Award from Brown University. RTS and DB were supported by NIH grant AI-16892. DB was also supported by Deutsche Forschungsgemeinschaft Grants BA 4890/1-1 and BA 4890/3-1. GL was supported by NIH 1R21 AI101393. CFN was supported by the Milstein Program in Translational Medicine and the TB Research Unit and NIH grant U19 AI111443.

## ABBREVIATIONS

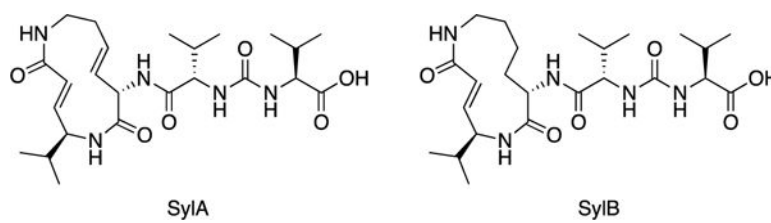
<b>Mtb</b>	Mycobacterium tuberculosis
<b>Mtb 20S</b>	Mycobacterium tuberculosis 20S proteasome
<b>SyIA</b>	syringolin A
<b>SyIB</b>	syringolin B
<b>CFU</b>	colony forming units

## References

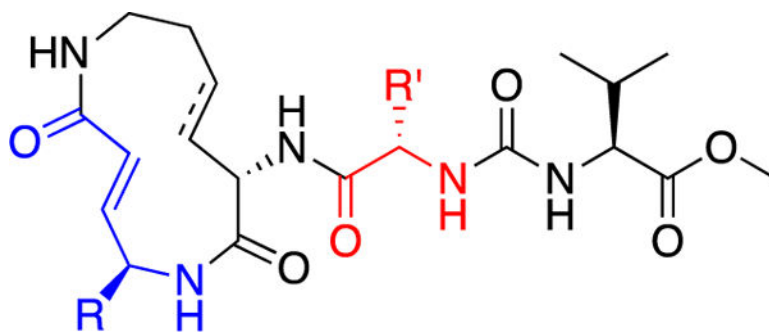
1. World Health Organization. Global Tuberculosis Report. 2015
2. Ma Z, Lienhardt C, McIlleron H, Nunn AJ, Wang X. Global Tuberculosis Drug Development Pipeline: The Need and the Reality. *Lancet*. 2010; 375:2100–2109. [PubMed: 20488518]
3. Darwin KH, Ehrst S, Gutierrez-Ramos JC, Weich N, Nathan CF. The Proteasome of Mycobacterium Tuberculosis Is Required for Resistance to Nitric Oxide. *Science*. 2003; 302:1963–1966. [PubMed: 14671303]
4. Gandotra S, Schnappinger D, Monteleone M, Hillen W, Ehrst S. In Vivo Gene Silencing Identifies the Mycobacterium Tuberculosis Proteasome as Essential for the Bacteria to Persist in Mice. *Nat Med*. 2007; 13:1515–1520. [PubMed: 18059281]
5. Striebel F, Hunkeler M, Summer H, Weber-Ban E. The Mycobacterial Mpa-Proteasome Unfolds and Degrades Pupylylated Substrates by Engaging Pups N-Terminus. *EMBO J*. 2010; 29:1262–1271. [PubMed: 20203624]
6. Lin G, Li D, Chidawanyika T, Nathan C, Li H. Fellutamide B Is a Potent Inhibitor of the Mycobacterium Tuberculosis Proteasome. *Arch Biochem Biophys*. 2010; 501:214–220. [PubMed: 20558127]
7. Lin G, Tsu C, Dick L, Zhou XK, Nathan C. Distinct Specificities of Mycobacterium Tuberculosis and Mammalian Proteasomes for N-Acetyl Tripeptide Substrates. *J Biol Chem*. 2008; 283:34423–34431. [PubMed: 18829465]
8. Lin G, Li D, de Carvalho LPS, Deng H, Tao H, Vogt G, Wu K, Schneider J, Chidawanyika T, Warren JD, Li H, Nathan C. Inhibitors Selective for Mycobacterial versus Human Proteasomes. *Nature*. 2009; 461:621–626. [PubMed: 19759536]
9. Lin G, Chidawanyika T, Tsu C, Warriar T, Vaubourgeix J, Blackburn C, Gigstad K, Sintchak M, Dick L, Nathan C. N,C-Capped Dipeptides with Selectivity for Mycobacterial Proteasome over Human Proteasomes: Role of S3 and S1 Binding Pockets. *J Am Chem Soc*. 2013; 135:9968–9971. [PubMed: 23782398]
10. Lin G, Hu G, Tsu C, Kunes YZ, Li H, Dick L, Parsons T, Li P, Chen Z, Zwickl P, Weich N, Nathan C. Mycobacterium Tuberculosis prcBA Genes Encode a Gated Proteasome with Broad Oligopeptide Specificity. *Mol Microbiol*. 2006; 59:1405–1416. [PubMed: 16468985]
11. Baumeister W, Walz J, Zühl F, Seemüller E. The Proteasome: Paradigm of a Self-Compartmentalizing Protease. *Cell*. 1998; 92:367–380. [PubMed: 9476896]
12. Hu G, Lin G, Wang M, Dick L, Xu RM, Nathan C, Li H. Structure of the Mycobacterium Tuberculosis Proteasome and Mechanism of Inhibition by a Peptidyl Boronate. *Mol Microbiol*. 2006; 59:1417–1428. [PubMed: 16468986]
13. Kisselev AF, Van Der Linden WA, Overkleeft HS. Proteasome Inhibitors: An Expanding Army Attacking a Unique Target. *Chem Biol*. 2012; 19:99–115. [PubMed: 22284358]
14. Singh J, Petter RC, Baillie TA, Whitty A. The Resurgence of Covalent Drugs. *Nat Rev Drug Discov*. 2011; 10:307–317. [PubMed: 21455239]
15. Krahn D, Ottmann C, Kaiser M. The Chemistry and Biology of Syringolins, Glidobactins and Cepafungins (Syrbactins). *Nat Prod Rep*. 2011; 28:1854–1867. [PubMed: 21904761]
16. Wäspi U, Misteli B, Hasslacher M, Jandrositz A, Kohlwein SD, Schwab H, Dudler R. The Defense-Related Rice Gene Pir7b Encodes an Alpha/beta Hydrolase Fold Protein Exhibiting Esterase Activity towards Naphthol AS-Esters. *Eur J Biochem*. 1998; 254:32–37. [PubMed: 9652390]
17. Groll M, Schellenberg B, Bachmann AS, Archer CR, Huber R, Powell TK, Lindow S, Kaiser M, Dudler R. A Plant Pathogen Virulence Factor Inhibits the Eukaryotic Proteasome by a Novel Mechanism. *Nature*. 2008; 452:755–759. [PubMed: 18401409]
18. Dai C, Stephenson CRJ. Total Synthesis of Syringolin A. *Org Lett*. 2010; 12:3453–3455. [PubMed: 20597471]
19. Pirrung MC, Biswas G, Ibarra-Rivera TR. Total Synthesis of Syringolin A and B. *Org Lett*. 2010; 12:2402–2405. [PubMed: 20426399]

20. Totaro KA, Barthelme D, Simpson PT, Sauer RT, Sello JK. Substrate-Guided Optimization of the Syringolins Yields Potent Proteasome Inhibitors with Activity against Leukemia Cell Lines. *Bioorganic Med Chem.* 2015; 23:6218–6222.
21. Clerc J, Groll M, Illich DJ, Bachmann AS, Huber R, Schellenberg B, Dudler R, Kaiser M. Synthetic and Structural Studies on Syringolin A and B Reveal Critical Determinants of Selectivity and Potency of Proteasome Inhibition. *Proc Natl Acad Sci.* 2009; 106:6507–6512. [PubMed: 19359491]
22. Opoku-Ansah J, Ibarra-Rivera TR, Pirrung MC, Bachmann AS. Syringolin B-Inspired Proteasome Inhibitor Analogue TIR-203 Exhibits Enhanced Biological Activity in Multiple Myeloma and Neuroblastoma. *Pharm Biol.* 2012; 50:25–29. [PubMed: 22196580]
23. Ibarra-Rivera TR, Opoku-Ansah J, Ambadi S, Bachmann AS, Pirrung MC. Syntheses and Cytotoxicity of Syringolin B-Based Proteasome Inhibitors. *Tetrahedron.* 2011; 67:9950–9956.
24. Li H, O'Donoghue AJ, van der Linden WA, Xie SC, Yoo E, Foe IT, Tilley L, Craik CS, da Fonseca PCA, Bogoy M. Structure- and Function-Based Design of Plasmodium-Selective Proteasome Inhibitors. *Nature.* 2016; 530:233–236. [PubMed: 26863983]

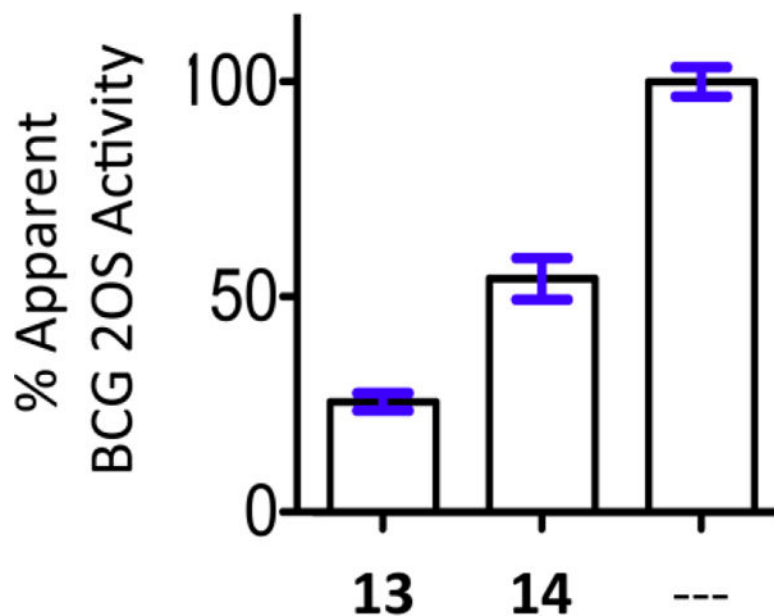




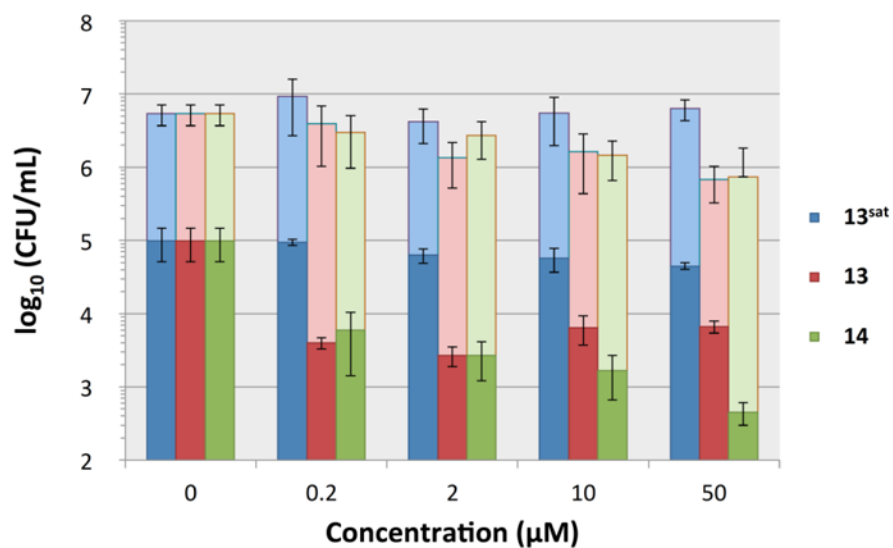
**Figure 1.** Chemical structures of syringolin A (SylA) and syringolin B (SylB) proteasome inhibitors.<sup>15</sup>



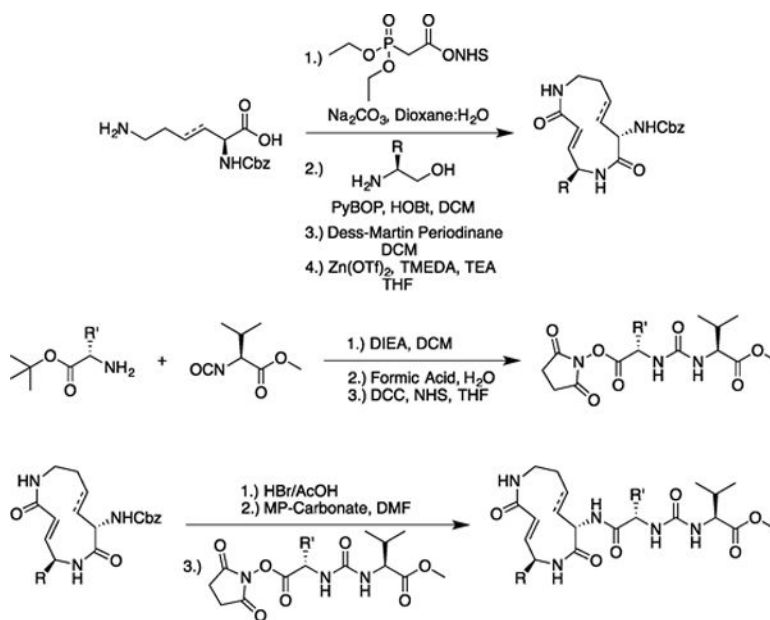
**Figure 2.** Structural model for proteasome substrate mimicry by the syringolins. Substituents at R and R' correspond to P1 and P3 residues of a peptide substrate, respectively.



**Figure 3.** Evaluating the cell permeability and activity of selective *Mtb* 20S inhibitors using *M. bovis* BCG. Apparent activity reflects proteasome-activity observed in lysates from the treated and untreated cultures. The proteasome activity observed in the untreated sample was set as 100%. The experiments were performed in triplicate. See supporting information for experimental protocols.



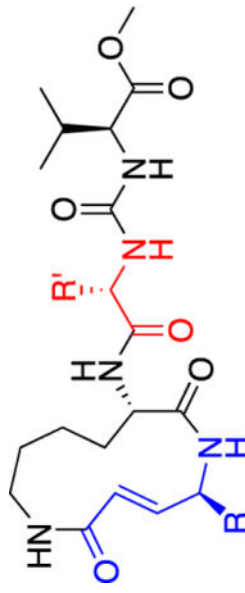
**Figure 4.** *Mtb* nitric-oxide stress assays for compound **14**. 0 µM experiment indicates CFU/mL value of DMSO control experiment. The lightly colored bars show CFU counts in assays lacking NaNO<sub>2</sub>. Assays were performed in triplicate. See supporting information for protocol.



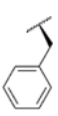



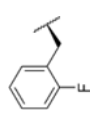
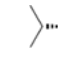
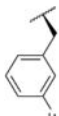

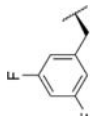
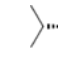
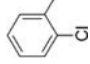
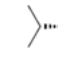


**Scheme 1.**  
Synthesis of syringolin analogs.<sup>18–20</sup>

The second-order rate constants for inhibition, species-selectivity, and structures of syringolin analogs that vary with respect substituents at the R and R' positions.

**Table 1**



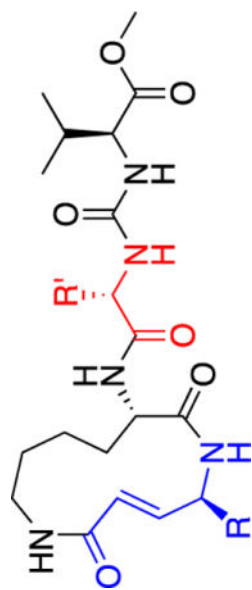
Compound	R	R'	<i>Hs</i> 20S $k_{in}/K_i$ ( $M^{-1}s^{-1}$ )	<i>Mtb</i> 20S $k_{in}/K_i$ ( $M^{-1}s^{-1}$ )	<i>Mtb</i> 20S $k_{in}/K_i$ / <i>Hs</i> 20S $k_{in}/K_i$
1			781	4.60	0.006
2			1913	85.8	0.045
3			188	16.8	0.090
4			1591	123	0.077
5			2471	157	0.064
6			1580	172	0.109
7			736	169	0.230

Author Manuscript

Author Manuscript

Author Manuscript

Author Manuscript



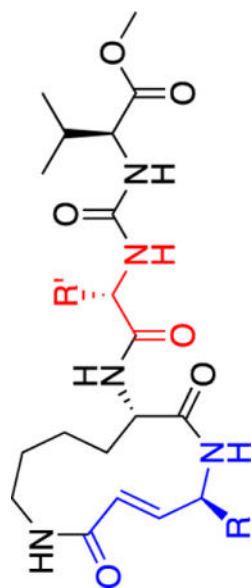
Compound	R	R'	<i>Hs</i> 20S $k_{in}/K_i$ ( $M^{-1}s^{-1}$ )	<i>Mtb</i> 20S $k_{in}/K_i$ ( $M^{-1}s^{-1}$ )	<i>Mtb</i> 20S $k_{in}/K_i$ <i>Hs</i> 20S $k_{in}/K_i$
8			1528	123	0.081
9			1214	101	0.083
10			636	89.6	0.141
11			1321	141	0.106
12			905	694	0.767
13			2.40	79.5	33.4
14		H	13.6	1013	74.3
15 <sup>[a]</sup>		H	71.5	1815	25.4

Author Manuscript

Author Manuscript

Author Manuscript

Author Manuscript



Compound	R	R'	<i>Hs</i> 20S $k_{in}/K_i$ ( $M^{-1}s^{-1}$ )	<i>Mb</i> 20S $k_{in}/K_i$ ( $M^{-1}s^{-1}$ )	<i>Mb</i> 20S $k_{in}/K_i$ <i>Hs</i> 20S $k_{in}/K_i$
16			4305	2263	0.526
17			112	2466	22.1
18			7.21	33.5	4.64

Syntheses and characterization data of all compounds are described in the supporting information.

<sup>[a]</sup>Compound contains an unsaturated macrolactam similar to syringolin A. Data reflect experiments performed in triplicate.